Blockage Effects on Joint Information & Energy Transfer in Directional Ad-Hoc Networks

Constantinos Psomas and Ioannis Krikidis
KIOS Research Center for Intelligent Systems and Networks
Department of Electrical and Computer Engineering, University of Cyprus, Cyprus
e-mail: {psomas, krikidis}@ucy.ac.cy

***Abstract*—The impact of blockages in the performance of next generation wireless networks has recently attracted a lot of attention. In this case, the existence of blockages can provide performance gains as the aggregate interference at a receiver is reduced. Furthermore, the employment of directional antennas at the network's nodes can further boost the performance through the power gains which antenna directionality produces. However, the impact of blockages on wireless power transfer has not been investigated equally. In this paper, we consider a bipolar ad-hoc network where the nodes employ directional antennas and have simultaneous wireless information and power transfer capabilities. We study the effects of blockages and directionality on the energy harvested by a receiver and show that the performance gains from the existence of blockages can be adjusted in order to increase the average harvested energy.**

***Index Terms*—SWIPT, power splitting, blockages, sectorized antennas, stochastic geometry.**

I. Introduction

Energy harvesting is considered an important aspect in next generation communication networks [1], since the harvested energy can either be used to reduce the network's dependence on the main power grid or can provide self-sustainability to low-powered networks (e.g. sensor networks). Traditional energy harvesting schemes from natural resources can be efficient but have a high level of uncertainty and uncontrollability. Therefore, energy harvesting from radio frequency (RF) signals has been recently proposed as an alternative. In particular, simultaneous wireless information and power transfer (SWIPT) is a new communication paradigm, where a wireless device can obtain both information and energy from the received RF signal [2]. Although information theoretic studies ideally assume that a receiver is able to decode information and harvest energy independently from the same signal [3], this approach is not feasible due to practical limitations. So to make SWIPT possible, the received RF signal needs to be split into two parts, one for information transfer and another for energy harvesting. The partitioning of the signal can be done in the time, power, antenna or space domain [4].

The SWIPT technology has been extensively studied in the literature for various scenarios. In [2], the authors study SWIPT in a point-to-point multiple-input multiple-output (MIMO) wireless system and derive the achievable rate-energy region for the time switching (TS) and power splitting (PS) technique. In the context of cooperative networks, the work in [5] considers multiple source-destination pairs which communicate via a relay which is powered by energy harvested from the received signals using the PS protocol; the authors investigate different power allocation policies for the relay transmissions to the destinations. Furthermore, in [6] the authors study the impact on the system's performance of a relay which employs full-duplex transmission and harvests energy from the received signals using the TS protocol.

As the effect of path-loss plays an important role in the performance of a communication system, stochastic geometry has been used to study SWIPT from a large-scale perspective. In [7], an uplink cellular network is studied where power beacons are deployed to wirelessly transfer energy to devices; the authors derive the trade-offs between the transmit power and density of both the devices and the power beacons. The work in [8] considers a network with multiple source-destination pairs where the receivers employ the PS method for SWIPT and the network's performance is derived under two protocols: non-cooperative and cooperative. Recently, several stochastic geometry studies have appeared which investigate the impact of blockages in the performance of wireless networks. One of the first studies was given by [9] where the authors provide an analytical framework for the analysis of blockages in cellular network with millimeter waves. In [10], the authors study how blockages affect heterogeneous cellular networks where the base stations from different tiers have the ability to cooperate. Moreover, the work in [11] considers blockages in a cellular network with SWIPT capabilities and investigates the impact of millimeter waves on RF energy harvesting.

The motivation of this paper is to study how blockages can positively affect the energy harvested by a receiver. We consider a bipolar ad-hoc network with blockages where the nodes employ sectorized directional antennas and the receivers implement SWIPT with the PS method. In such a scenario, the outage probability of a receiver is improved due to the use of directional antennas and also due to the existence of blockages which decrease the overall interference at the receiver. We show how these performance gains can be "sacrificed" in order to increase the harvested energy by a proper selection of the PS parameter. We derive analytical expressions and provide

This work was supported by the Research Promotion Foundation, Cyprus, under the project FUPLEX with pr. no. CY-IL/0114/02.

978-0-9928-6265-7/16/$31.00 ©2016 IEEE

numerical results for the outage probability and average harvested energy for the optimal split with respect to the other parameters of the network. The rest of the paper is organized as follows. Section II presents the network model together with the antenna, channel and SWIPT models. Section III provides the main analytical results of the paper and in Section IV we present the numerical results which validate our assumptions. Finally, the conclusion of the paper is given in Section V.

Notation: $\mathbb{R}^d$ denotes the d-dimensional Euclidean space, $\mathbb{P}[X]$ denotes the probability of the event X and $\mathbb{E}[X]$ represents the expected value of X, $\Gamma(x)$ denotes the Gamma function, $\csc(\theta)$ is the cosecant of angle θ.

II. System model

A. Network model

We consider a large-scale bipolar ad-hoc wireless network consisting of a random number of transmitter-receiver pairs. The transmitters form a homogeneous Poisson point process (PPP) $\Phi = \{x_i : i = 1, 2, \dots\}$ of density λ in the Euclidean plane $\mathbb{R}^2$, where $x_i \in \mathbb{R}^2$ denotes the location of the i-th transmitter. Each transmitter x_i has a unique receiver at a distance d_0 in some random direction [6]. The time is considered to be slotted and in each time slot all the transmitters are active without any coordination or scheduling. We consider a receiver located at the origin and its associated transmitter x_0 located at a distance d_0 from the origin in some random direction. We perform our analysis for this typical receiver but, according to Slivnyak's Theorem [12], our results hold for any receiver in the network. The considered network is assumed to include blockages, e.g. buildings, which we are modeled by a line segment process of two dimensional lines with random lengths and orientations. The center points of the lines are distributed according to a PPP of density ρ in the Euclidean plane [9]. Then, the probability of having a line-of-sight (LOS) and a non-line-of-sight (NLOS) path at a distance d between a transmitter and a receiver is $p_L(d) = \exp(-\beta d)$ and $p_N(d) = 1 - p_L(d)$ respectively, where β is a non-negative constant defined by $\beta = \frac{2\rho\mathbb{E}[L]}{\pi}$ and where L denotes the length of the blockages [9].

B. Antenna model

All nodes are assumed to be equipped with the same number of sectorized antennas. We define as M the number of directional transmit/receive antennas employed at a node, so $M = 1$ refers to the omni-directional case. The main and side lobes of each antenna are approximated by a circular sector. It is assumed that the antenna gain of the main lobe is $G = \frac{M}{1+\gamma(M-1)}$ where γ is the ratio of the side lobe level to the main lobe level and so the antenna gain of the side lobe is $H = \gamma G$ [13]. The antenna directivity gain of a link changes according to whether a transmission occurs towards or away from the main or side lobe of a receiver. Using similar arguments as in [13], there are three possible antenna directivity gains between a receiver and the interfering transmitters: between main lobes, between side lobes and between a main and a side lobe. Therefore, the antenna directivity gain for each case is given by $\Gamma_i = \{G^2, GH, H^2\}$ and occurs with probability $p_i = \left\{\frac{1}{M^2}, \frac{2(M-1)}{M^2}, \frac{(M-1)^2}{M^2}\right\}$, $i \in \{1, 2, 3\}$. As for the direct links, we assume that the transmitters are perfectly aligned with their associated receivers, i.e. the antenna directivity gain equals to G^2.

C. Channel model

We assume that all wireless links suffer from both small-scale block fading and large-scale path-loss effects. The fading is considered to be Rayleigh distributed so the power of the channel fading is an exponential random variable with unit variance. We denote by h_i the channel coefficient for the link between the i-th transmitter and the typical receiver. Moreover, all wireless links exhibit additive white Gaussian noise (AWGN) with variance σ^2. The path-loss model assumes that the received power is proportional to $(1+d_i^\alpha)^{-1}$ where d_i is the Euclidean distance from the origin to the i-th transmitter and $\alpha > 2$ is the path-loss exponent. We consider this bounded path-loss model as it ensures that the mean interference is finite.

D. Joint information & energy transfer

It is assumed that the transmitters have a continuous power supply, such as a battery or the power grid, and transmit with the same power P_t. Each receiver has SWIPT capabilities and so it can decode the information and also harvest energy from the received signal simultaneously. The SWIPT technology is employed with the PS method such that the received signal is split into two parts: one is converted to a baseband signal for information decoding and the other is directed to the rectenna for energy harvesting and storage. Let $0 < v \leq 1$ denote the PS parameter for each receiver, i.e. $100v\%$ of the received power is used for decoding while the remaining power is inputted to the energy harvesting circuit. During the baseband conversion phase, additional circuit noise is presented due to the phase-offsets and the circuit's non-linearities which is modeled as an AWGN with zero mean and variance σ_C^2.

As discussed in Section II-C, there are three possible ways to characterize the power gain of a received signal at the typical receiver. Consequently, this produces three thinning processes Φ_i with density $\xi_i = \lambda p_i$, $i \in \{1, 2, 3\}$ [12]. Therefore, based on the PS technique considered, the signal-to-interference-plus-noise ratio (SINR) at the typical receiver can be written as

$$\mathrm{SINR} = \frac{v P_t h_0 \Gamma_1 (1 + d_0^\alpha)^{-1}}{v(\sigma^2 + P_t \mathcal{I}) + \sigma_C^2} \tag{1}$$

where

$$\mathcal{I} = \sum_{i \in \{1,2,3\}} \sum_{x_j \in \Phi_i} h_j \Gamma_i (1 + d_j^\alpha)^{-1}, j > 0, \tag{2}$$

is the aggregate interference at the typical receiver and α takes the values α_L and α_N with probability $p_L(d)$ and $p_N(d)$ respectively. A successful decoding requires that the SINR at the receiver is at least equal to a certain detection threshold θ.

On the other hand, RF energy harvesting is a long term operation and is expressed in terms of average harvested energy [6]. Since $100(1-v)\%$ of the received energy is used for rectification, the average energy harvested at the typical receiver is expressed as

$$E(v) = \zeta\, \mathbb{E}\left[(1-v)P_t\left(h_0\Gamma_1(1+d_0^{\alpha})^{-1}+\mathcal{I}\right)\right], \quad (3)$$

where $0 < \zeta \leq 1$ denotes the conversion efficiency from the RF signal to direct-current voltage. For the sake of simplicity, we will assume throughout the paper that $\zeta = 1$. Any potential RF energy harvesting from the AWGN noise is considered to be negligible.

III. SWIPT Performance with Blockages

In this section, we present the main results of our proposed model. Specifically, we analytically derive the outage probability, i.e. $\mathbb{P}[\text{SINR} < \theta]$, and also the expected harvested energy at the typical receiver.

Lemma 1. *The Laplace transform of the interference $\mathcal{I}$ at the typical receiver evaluated at s is given by*

$$\mathcal{L}_{\mathcal{I}}(s) = \prod_{i\in\{1,2,3\}} \exp\left(-2\pi\xi_i \int_0^{\infty} (1-c_L(r)-c_N(r))\, r dr\right), \quad (4)$$

where $c_x(r) = \frac{1+r^{\alpha_x}}{s\Gamma_i+1+r^{\alpha_x}} p_x(r)$, $x \in \{L,N\}$.

Proof: The Laplace transform of the interference $\mathcal{I}$ is evaluated as follows

$$\begin{aligned}
\mathcal{L}_{\mathcal{I}}(s) &= \mathbb{E}\left[\exp\left(-s\sum_{i\in\{1,2,3\}}\sum_{x_j\in\Phi_i}\frac{h_j\Gamma_i}{1+d_j^{\alpha}}\right)\right] \\
&= \prod_{i\in\{1,2,3\}} \mathbb{E}\Bigg[\prod_{x_j\in\Phi_i} \mathbb{E}_{h_j}\left[\exp\left(-s\frac{h_j\Gamma_i}{1+d_j^{\alpha_L}}\right)\right] p_L(d_j) \\
&\qquad + \mathbb{E}_{h_j}\left[\exp\left(-s\frac{h_j\Gamma_i}{1+d_j^{\alpha_N}}\right)\right] p_N(d_j)\Bigg] \\
&= \prod_{i\in\{1,2,3\}} \mathbb{E}\Bigg[\prod_{x_j\in\Phi_i} \frac{p_L(d_j)}{1+s\Gamma_i(1+d_j^{\alpha_L})^{-1}} \\
&\qquad + \frac{p_N(d_j)}{1+s\Gamma_i(1+d_j^{\alpha_N})^{-1}}\Bigg],
\end{aligned}$$

where the expectation term is given by

$$\exp\Bigg(-2\pi\xi_i\int_0^{\infty}\Bigg(1-\frac{p_L(r)}{1+s\Gamma_i(1+r^{\alpha_L})^{-1}} - \frac{p_N(r)}{1+s\Gamma_i(1+r^{\alpha_N})^{-1}}\Bigg) r dr\Bigg),$$

which follows from the probability generating functional of a PPP [12]. By setting $c_x(r) = \frac{1+r^{\alpha_x}}{s\Gamma_i+1+r^{\alpha_x}} p_x(r)$, $x \in \{L,N\}$ the result follows. ∎

Theorem 1. *The outage probability of the typical receiver is*

$$\begin{aligned}
P_o(v,\beta) = 1 &- p_L(d_0)\exp\left(-\frac{s_L}{P_t}\left(\sigma^2+\frac{\sigma_C^2}{v}\right)\right)\mathcal{L}_{\mathcal{I}}(s_L) \\
&- p_N(d_0)\exp\left(-\frac{s_N}{P_t}\left(\sigma^2+\frac{\sigma_C^2}{v}\right)\right)\mathcal{L}_{\mathcal{I}}(s_N), \quad (5)
\end{aligned}$$

where $s_x = \frac{\theta(1+d_0^{\alpha_x})}{\Gamma_1}$, $x \in \{L,N\}$ and $\mathcal{L}_{\mathcal{I}}(s_x)$ is given by Lemma 1.

Proof: Since h_0 is an exponential random variable with unit variance, we have

$$\begin{aligned}
P_o(v,\beta) &= 1 - \mathbb{P}\left[\text{SINR} > \theta\right] \\
&= 1 - \exp\left(-\frac{\theta(1+d_0^{\alpha})}{\Gamma_1 P_t}\left(\sigma^2+\frac{\sigma_C^2}{v}\right)\right)\mathcal{L}_{\mathcal{I}}\left(\frac{\theta(1+d_0^{\alpha})}{\Gamma_1}\right). \quad (6)
\end{aligned}$$

The result then follows by taking into account the LOS and NLOS cases. ∎

Theorem 2. *The average harvested energy by the typical receiver is given by*

$$E(v) = (1-v)P_t\left(\Gamma_1\frac{p_L(d_0)}{1+d_0^{\alpha_L}} + \Gamma_1\frac{p_N(d_0)}{1+d_0^{\alpha_N}} + \Psi\right), \quad (7)$$

where

$$\Psi = 2\pi\sum_{i\in\{1,2,3\}}\xi_i\Gamma_i\int_0^{\infty}\left(\frac{p_L(r)}{1+r^{\alpha_L}} + \frac{p_N(r)}{1+r^{\alpha_N}}\right) r dr. \quad (8)$$

Proof: Similarly to [8], using Campbell's theorem for the expectation of a sum over a point process [12] and the fact that $\mathbb{E}(h_i) = 1$ for all i, we get from (3),

$$E(v) = (1-v)P_t\left(\Gamma_1\frac{p_L(d_0)}{1+d_0^{\alpha_L}} + \Gamma_1\frac{p_N(d_0)}{1+d_0^{\alpha_N}} + \mathbb{E}[\mathcal{I}]\right), \quad (9)$$

where,

$$\begin{aligned}
\mathbb{E}[\mathcal{I}] &= \mathbb{E}\left[\sum_{i\in\{1,2,3\}}\sum_{x_j\in\Phi_i}(1+d_j^{\alpha})^{-1}\right] \\
&= 2\pi\sum_{i\in\{1,2,3\}}\xi_i\Gamma_i\int_0^{\infty}\left(\frac{p_L(r)}{1+r^{\alpha_L}} + \frac{p_N(r)}{1+r^{\alpha_N}}\right) r dr,
\end{aligned}$$

which proves the theorem. ∎

Next, we consider two asymptotic cases, namely $M \to \infty$ and $\beta \to \infty$. When $M \to \infty$ we have $\Gamma_i \to \left\{\frac{1}{\gamma^2}, \frac{1}{\gamma}, 1\right\}$ and $p_i \to \{0,0,1\}$, in which case the Laplace transform in Lemma 1 changes to

$$\mathcal{L}_{\mathcal{I}}^{\infty}(s) = \exp\left(-2\pi\lambda\int_0^{\infty}(1-c_L(r)-c_N(r))\, r dr\right), \quad (10)$$

with $c_x(r) = \frac{p_x(r)}{1+s(1+r^{\alpha_x})^{-1}}$; the term Ψ in Theorem 2 changes to

$$\Psi^{\infty} = 2\pi\lambda\int_0^{\infty}\left(\frac{p_L(r)}{1+r^{\alpha_L}} + \frac{p_N(r)}{1+r^{\alpha_N}}\right) r dr. \quad (11)$$

Similarly, for the case $\beta \to \infty$, all paths are NLOS so we have $p_L(r) \to 0$ and $p_N(r) \to 1$ which produces the following expressions,

$$\mathcal{L}_{\mathcal{I}}^{N}(s_N) = \prod_{i\in\{1,2,3\}} \exp\left(-2\pi\xi_i \int_0^\infty \frac{s_N\Gamma_i r}{s_N\Gamma_i + 1 + r^{\alpha_N}} dr\right)$$
$$= \prod_{i\in\{1,2,3\}} \exp\left(-\frac{2\pi^2\xi_i}{\alpha_N} s_N\Gamma_i (1+\Gamma_i s)^{\frac{2}{\alpha_N}-1} \csc\left(\frac{2\pi}{\alpha_N}\right)\right), \quad (12)$$

where $s_N = \frac{\theta(1+d_0^{\alpha_N})}{\Gamma_1}$; the term Ψ in Theorem 2 changes to

$$\Psi^N = 2\pi\lambda \sum_{i\in\{1,2,3\}} p_i\Gamma_i \int_0^\infty \frac{r}{1+r^{\alpha_N}} dr$$
$$= \frac{2\pi^2\lambda}{\alpha_N} \csc\left(\frac{2\pi}{\alpha_N}\right) \sum_{i\in\{1,2,3\}} p_i\Gamma_i, \quad (13)$$

which follows from using the transformation $u \leftarrow r^2$ and [14, 3.241]. The results of Theorem 1 and Theorem 2 change accordingly for each of the asymptotic cases.

We now formulate an optimization problem to find the optimal value of v which maximizes the average harvested energy under an outage constraint. An increase of the blockage density could result in a possible drop in outage probability. From a SWIPT point of view, this reduction can be exploited in order to re-evaluate the PS parameter v to increase the harvested energy whilst keeping the outage probability lower than a certain value. In other words, we would like to compute

$$\max_{v} \; E(v) \quad (14)$$
$$\text{subject to} \quad 0 < v \leq 1,$$
$$P_o(v,\beta) \leq \eta, \quad (15)$$

where η is an outage probability constraint. In order to maximize the average harvested energy at the receiver, it suffices to minimize v subject to the above constraints. This can be found by finding the root of the equation $P_o(v,\beta) = \eta$. Due to the complexity of the expressions, finding the root of the equation is non-trivial but can be derived using numerical methods such as the bisection search or Newton's method. For the asymptotic case $\beta \to \infty$, the solution can be evaluated due to the simplified expressions and is given by

$$v = -\frac{\sigma_C^2}{\frac{P_t}{s_N} \ln\left[\frac{1-\eta}{\mathcal{L}_{\mathcal{I}}^{N}(s_N)}\right] - \sigma^2}. \quad (16)$$

In the next section we present the numerical results of our proposed model.

IV. Numerical Results

We provide numerical results to validate our proposed model and demonstrate the potential benefits from its implementation. Unless otherwise stated, the numerical results use $\lambda = 10^{-3}$, $\gamma = 0.3$, $d_0 = 5$ m, $\theta = 0$ dB, $\sigma^2 = 1$, $\sigma_C^2 = 1$, $v = 0.5$, $L = 10$ m, $\alpha_L = 2$ and $\alpha_N = 4$. The solutions to (14) were evaluated with the help of Mathematica which uses Newton's method. In Fig. 1, we show how the outage probability is affected by the blockage density and the number of sectorized antennas. Firstly, it is clear that, an increase in M decreases the outage probability regardless of the blockage density; this is expected as a larger M means larger antenna directivity gain and less interference. Now the effect of the blockage density on the performance of the receiver depends on the system's other parameters. A small value of d_0 ensures that an increase in blockage density will improve the outage probability since the direct link will most probably be in LOS and the interfering signals in NLOS. For larger values of d_0, the performance depends on the transmit power. For $P_t = 30$ dB the outage probability improves slightly for small values of ρ but the performance worsens as ρ increases. On the other hand, for $P_t = 50$ dB, the outage probability benefits from an increase in the blockage density. Theoretical curves (dashed lines) perfectly match the numerical results (markers) and validate our analysis. Moreover, all curves converge to the asymptotic case which validates (12). In Fig. 2, we plot the optimal v obtained by (14) with respect to the blockage density ρ for different values of θ. We consider the case $M \to \infty$ and we let the outage constraint in (15) to be $P_o(0.5, \frac{2\rho\mathbb{E}[L]}{\pi})$ with $\rho = 10^{-4}$ and $L = 10$ m. It is obvious that for $P_t = 50$ dB and for values of $\rho > 10^{-4}$, the PS parameter v can be reduced significantly compared to the initial PS value of 0.5. For large values of ρ, v increases but is still much smaller than the initial value. The reason for this increase is due to the fact that for large values of ρ the direct link between the receiver and its transmitter is likely to be in NLOS. Finally, a larger value of θ, in this case $\theta = 10$ dB, provides a lower v compared to $\theta = 0$ dB. Larger threshold values provide a higher outage probability and so the benefit of interference reduction due to the existence of blockages is more obvious in these cases. Finally, in Fig. 3, we illustrate how the average

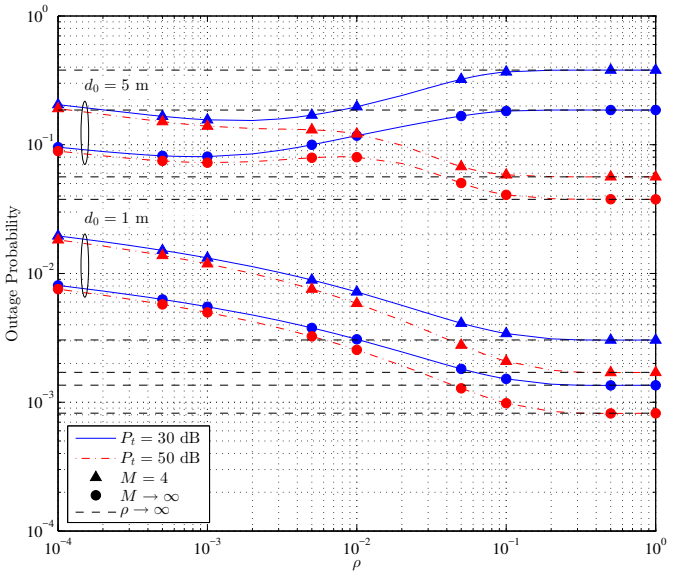

Fig. 1. Outage probability versus blockage density ρ; $v = 0.5$, $\theta = 0$ dB.

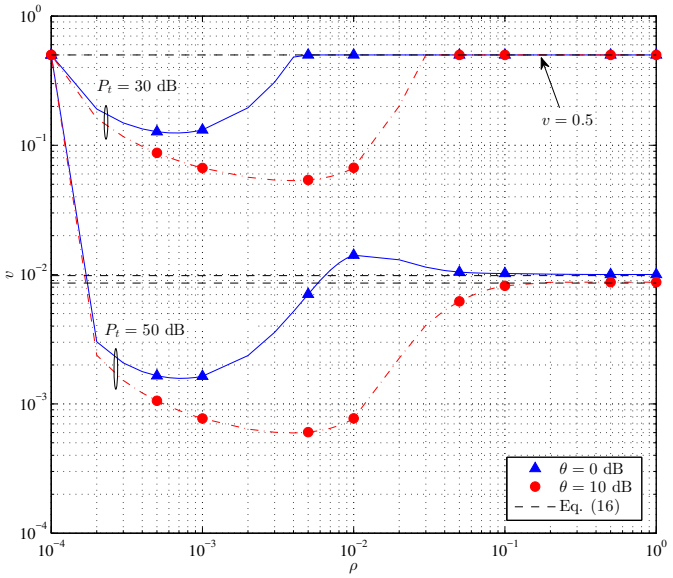

Fig. 2. Optimal v versus the blockage density ρ; $\gamma = 0.3$, $d_0 = 5$ m, $M \to \infty$.

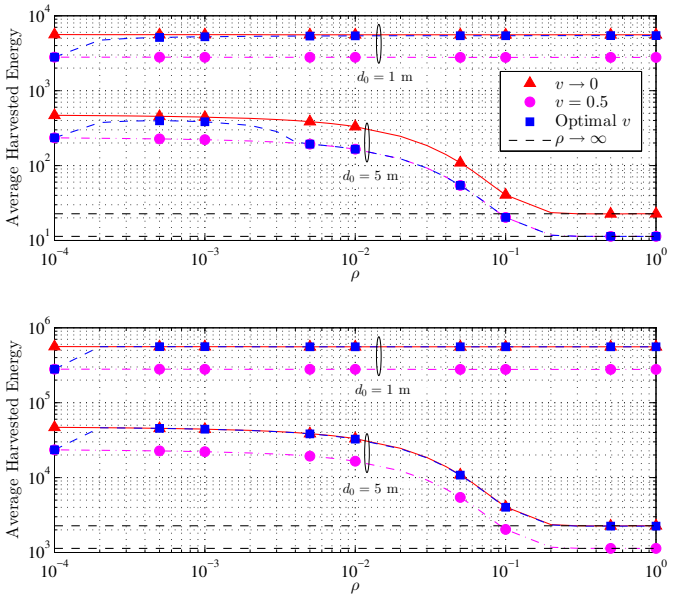

Fig. 3. Average harvested energy versus ρ with $P_t = 30$ dB (upper plot) and $P_t = 50$ dB (lower plot); $M \to \infty$, $\gamma = 0.3$, $\theta = 0$ dB.

harvested energy changes with respect to the blockage density ρ. The case where v remains constant as the blockage density increases is compared to the case where v is adjusted using the optimal values of v given in Fig. 2. Similar observations to above apply. For $d_0 = 1$ m and $P_t = 50$ dB, more energy is harvested since the direct link is much stronger compared to the cases $d_0 = 5$ m and $P_t = 30$ dB. When $\rho \to \infty$, all links are in NLOS which provides less harvested energy from both the direct and the interfering signals. In this case, the average harvested energy converges to a constant floor given by Theorem 2 and (13). Lastly, we plot the upper bound for the harvested energy, i.e. the case $v \to 0$. It's obvious that the adjustment of v by (14) can match the upper bound under certain parameters.

V. Conclusion

In this paper we investigated the impact of blockages on the harvested energy in wireless ad-hoc networks. We considered a bipolar ad-hoc network with sectorized directional antennas and SWIPT capabilities. We showed that an increase in the density of the blockages can be useful in order to adjust the PS parameter accordingly while satisfying an outage constraint in a network with smaller blockage density. We derived analytically the outage probability and the average harvested energy by modelling our considered network with spatial point processes and have presented numerical results to validate our assumptions. Our results provide the necessary insight in the design of SWIPT networks with the existence of blockages. Since the adjustment of the PS parameter in some cases can reach the upper bound of harvested energy, it provides the flexibility to design the network's parameters in such a way as to achieve specific quality of service constraints but also increase the harvested energy.

References

[1] I. Ahmed, M. M. Butt, C. Psomas, A. Mohamed, I. Krikidis, and M. Guizani, "Survey on energy harvesting communications: Challenges and opportunities for radio resource allocation," *Elsevier J. Comput. Networks*, vol. 88, pp. 234–248, Sept. 2015.

[2] R. Zhang and C. K. Ho, "MIMO broadcasting for simultaneous wireless information and power transfer," *IEEE Trans. Wireless Commun.*, vol. 12, pp. 1989–2001, May 2013.

[3] P. Grover and A. Sahai, "Shannon meets Tesla: Wireless information and power transfer," in *Proc. IEEE Int. Symp. Inf. Theory*, Austin, USA, June 2010, pp. 2363–2367.

[4] I. Krikidis, S. Timotheou, S. Nikolaou, G. Zheng, D. W. K. Ng, and R. Schober, "Simultaneous wireless information and power transfer in modern communication systems," *IEEE Commun. Mag.*, vol. 52, pp. 104–110, Nov. 2014.

[5] Z. Ding, S. M. Perlaza, I. Esnaola, and H. V. Poor, "Power allocation strategies in energy harvesting wireless cooperative networks," *IEEE Trans. Wireless Commun.*, vol. 13, pp. 846–860, Jan. 2014.

[6] C. Zhong, H. A. Suraweera, G. Zheng, I. Krikidis, and Z. Zhang, "Wireless information and power transfer with full duplex relaying," *IEEE Trans. Commun.*, vol. 62, pp. 3447–3461, Jan. 2014.

[7] K. Huang and V. K. N. Lau, "Enabling wireless power transfer in cellular networks: Architecture, modeling and deployment," *IEEE Trans. Wireless Commun.*, vol. 13, pp. 902–912, Feb. 2014.

[8] I. Krikidis, "Simultaneous information and energy transfer in large-scale networks with/without relaying," *IEEE Trans. Commun.*, vol. 62, pp. 900–912, March 2014.

[9] B. Tianyang, R. Vaze, and R. W. Heath, "Analysis of blockage effects on urban cellular networks," *IEEE Trans. Wireless Commun.*, vol. 13, pp. 5070–5083, 2014.

[10] D. Maamari, N. Devroye, and D. Tuninetti "Coverage in mmWave cellular networks with base station cooperation," *IEEE Trans. Wireless Commun.*, vol. 15, pp. 2981–2994, Jan. 2016.

[11] T. A. Khan, A. Alkhateeb, and R. W. Heath, "Millimeter wave energy harvesting," *IEEE Trans. Wireless Commun.*, to be published, 2016 [Online]. Available: http://arxiv.org/pdf/1509.01653v1.pdf

[12] M. Haenggi, *Stochastic geometry for wireless networks*, Cambridge Uni. Press, 2013.

[13] A. M. Hunter, J. G. Andrews, and S. Weber, "Transmission capacity of ad hoc networks with spatial diversity," *IEEE Trans. Wireless Commun.*, vol. 7, pp. 5058–5071, Dec. 2008.

[14] I. S. Gradshteyn and I. M. Ryzhik, *Table of integrals, series, and products*, Elsevier, 2007.